JOURNAL OF MATERIALS SCIENCE 11 (1976) 823–835

Single groove double cantilever beam fracture specimens versus Dugdale specimens for estimating shear lip propagation energies: BPA polycarbonate

R. P. KAMBOUR, S. MILLER
General Electric Company, Corporate Research and Development, Synthesis & Characterization Branch, Schenectady, New York, USA

Cracks in double cantilever beam specimens with single side grooves (S-G DCB) exhibit crack tip plastic zones that mimic closely the plastic zones that produce shear lips in mixed mode crack propagation in thick specimens of polycarbonate. In both the S-G DCB plastic zone and the shear lip the plastic strain is 30%. The S-G DCB strain energy release rate is a linear function of thickness, as a result of the fact that the cross-sectional area of the plastic zone increases linearly with the square of the net section thickness while the plastic strain in the zone is independent of thickness. In Dugdale specimens the thickness dependence of G_C is different from and more complex than that in the S-G DCB specimens. For each geometry G_C starts at zero thickness, but for Dugdale specimens rises eight times faster with the thickness at first. This greater thickness dependence of G_C in the Dugdale specimens arises from a greater dependence of zone cross-sectional area on thickness and a greater zone plastic strain (50 to 60% mostly). Other advantages of S-G DCB specimens versus Dugdale specimens in assessing ductile fracture are discussed.

1. Occurrence of shear lip formation in ductile materials

The development of shear lips during cracking propagation in solids is a phenomenon widely said to occur when certain conditions are met: (1) the material must be capable of undergoing plane stress yielding; (2) in a thick specimen the constraints imposed by a pre-existent notch or crack are sufficient to allow plane strain yielding at most in the specimen interior.

1.1. Metals

Shear lips in metals are frequently discussed in the context of "pop-in" failure of thick specimens containing sharp single edge notches (e.g. [1] p. 135). With increase in machine displacement as in a three-point bend test for example, a load is reached at which a crack (usually termed a plane strain crack) suddenly "pops" into the specimen for a distance. The associated load maximum and the notch depth are often used (with the modulus) to calculate the plane stress strain energy release rate G_{IC}. Depending on the material, the specimen geometry and the test conditions further machine displacement will cause the "plane strain" crack to propagate to some greater depth before cracks begin to propagate in the surface ligaments. With materials that can exhibit high ultimate tensile elongations this depth tends to be large compared to the width of the surface ligament.

The failure of each of the two surface ligaments is often said to be a plane stress failure the mechanics of which can be characterized by tensioning a thin sheet of the material containing a central slit or edge slits (e.g. [1] Chs. 2 and 3). Long thin yield zones often grow from the slit ends. Measurement of the lengths of the crack and yield zones up to the point of rupture allows use of a Dugdale model [2, 3] to calculate a value of G_C the strain energy release rate for crack propagation. If the

yield zone dimension in the stress direction is great enough compared to the sheet thickness (e.g. 4 times as great) the zone can be said to exist under plane stress conditions (i.e. $\sigma_{zz} = 0$ where z is the direction normal to the sheet surface) and the value of G_C obtained is usually termed the plane stress strain energy release rate.

The value of G_C obtained has been found to depend on the thickness of the specimen. With many metals (e.g. 7075-T6 aluminium alloy) G_C is known to rise linearly with thickness from an extrapolated value of zero at zero thickness [1, 4, 5]. Only the onset of the plane strain fracture mode in the specimen interior halts the rise in energy required to propagate failure. According to Tetelman and McEvily the dependence of plane stress G_C on thickness is related to the "gauge" length of the plastic zone in the stress direction – a length which is essentially equal to specimen thickness*. This relationship depends on the assumption that post-yield plastic deformation is confined to the material in this zone. This point will be re-examined shortly.

In any case following the appearance of the plane strain mode G_C drops with increasing thickness and asymptotically approaches a level value (G_{IC}) in very thick sheet.

With metals rough estimates of shear lip sizes can be made if the plane strain stress intensity factor K_{IC} and the size of the associated plastic zone are known. With increase in specimen thickness pop-in failure can be first expected at a thickness

$$\tau_0 \geqslant \frac{1}{\pi}\left(\frac{K_{IC}}{\sigma y}\right)^2 = 2R \qquad (1)$$

where R is the plastic zone radius (e.g. [1] pp. 137–8). Tetelman and McEvily suggest that the shear lip size will equal or exceed τ_0 at all greater sheet thicknesses, and cite examples of both kinds of behaviour.

However, precise estimates of shear lip sizes appear difficult to make because there are a number of aspects of the two modes of failure and their interaction that are not sufficiently well understood. For example, Weiss and Yukawa [6] point out that virtually nothing is known about the specific details of the abruptness of the change from plane stress to plane strain plastic behaviour. According to Knott [5] it is quite possible that at the onset of pop-in fracture the value of σ_{zz} in the median plane of the sheet may not have reached its full plane strain magnitude although it has induced enough tri-axiality to change the fracture mode. Under this condition the pop-in value of G_C may not correspond to G_{IC}. Furthermore Knott points out the difficulty in determining the dependence of σ_{zz} on z from the sheet surface inward, particularly when plastic deformation occurs at the crack or notch tip.

1.2. Thermoplastics

Shear lip formation although observable in many organic thermoplastics has been discussed in the literature in a few cases only: fatigue crack propagation in polycarbonate [7], pop-in failure of polycarbonate [8], and low speed crack propagation in vinyl urethane polymers [9].

We have observed shear lip formation in half inch thick double cantilever beam specimens of BPA polycarbonate. In these the two conventional side grooves [10] were cut only a short way along the specimen. The plane strain crack was initiated at the conventional swallow tail and caused to propagate under cyclic fatigue to the end of the grooved portion of the specimen. Under static loading, propagation beyond this point occurred in the specimen interiors but shear lips 0.05 in. wide in one case and 0.10 in. wide in another formed at each surface.

Shear lips were also produced in another more complex experiment that reflects conditions occasionally met in the field. An environmental stress crack was first propagated into a cleavage specimen using carbon tetrachloride which is a potent cracking agent for polycarbonate. The crack front was U-shaped (Fig. 1) with the crack at the surfaces lagging that in the center of the specimen by about 3/4 in. The crack was allowed to dry for a few weeks and the wedge then reinserted. A small amount of plane strain propagation (i.e. craze formation and breakdown) occurred in the specimen interior. Each surface ligament, however, developed a bifurcated shear zone one-half above and one-half below the internal crack plane. Driving the wedge into the specimen further caused the tips of these zones to propagate forward but spread apart simultaneously.

Data from which the energies of shear lip

* More recently, however, Knott [5] has reported that the mode of fracture in the thin sheets of 7075–T6 aluminium alloy is more nearly Mode III than Mode I. If so the Tetelman–McEvily rationale may not be applicable to this material.

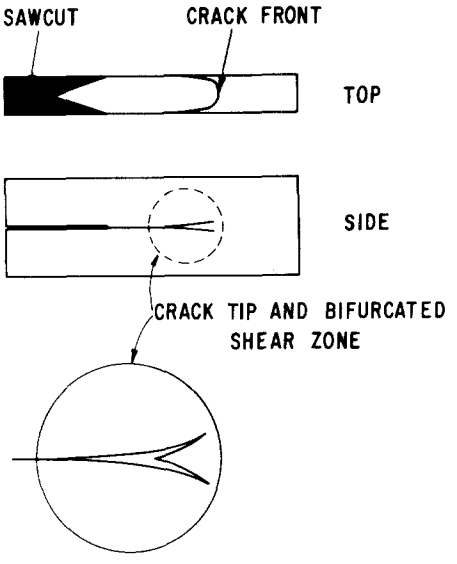

Figure 1 Diagrams of U-shaped crack in $\frac{1}{2}$in. thick polycarbonate specimen. Driving of wedge into sawcut produced slight advance of crack internally and pronounced bifurcated shear zones on each surface.

propagation might be even crudely estimated are very scarce. Brinson [11] has reported the results of Dugdale experiments with a single thickness of polycarbonate sheet (0.020 in.). Centre notched specimens were pulled to failure at a constant strain-rate. The lengths of the cracks and the thin yield zones beyond the crack tips were measured as a function of load. The data obtained fit the Dugdale model [2] and a value of G_C was calculated in the manner given by Goodier and Field [3]. However, as discussed below a strong thickness dependence exists for G_C in polycarbonate sheets as determined in Dugdale experiments.

In the course of studies here of ductile and brittle failure in polycarbonate systems it became desirable to have a better method of assessing shear lip formation energies than afforded by Dugdale specimens. There are several aspects of the Dugdale method that can make it inadequate for the determination of shear lip formation energies.

(1) The configuration of stresses on the ligament at the tip of the Dugdale slit in a thin sheet differs from that on the surface ligament beneath which is a deep plane strain crack as in Fig. 1. The whole of the Dugdale ligament is under plane stress since it is bounded by two essentially flat surfaces. However, in the latter case, the ligament will be under plane stress only at its one free surface; at the underlying crack the ligament will experience a stress state having a triaxial component greater than that corresponding to plane stress.

(2) In this study it was important to be able to determine the crack velocity dependence of shear lip energies. The conventional Dugdale specimen, however, can only give a value of G_C at the point of specimen instability, i.e. at a point where crack velocity is low but accelerating strongly. As with G_{IC} measurements the determination of the crack velocity dependence of G_C requires that a steady state plastic zone be established at a known, constant crack velocity.

(3) Dugdale analyses are most accurate in cases where the yield zones formed at the slit tips are long and thin, i.e. in shape the zone approximates an extension of the slit. In many cases the yield zones at the point of failure have other shapes, e.g. the bifurcated surface zone of Fig. 1.

(4) For plastics *a priori* estimates of shear lip size, and thus shear lip energies, appear to be even more uncertain than in metals. In metals the plastic flows involved in plane stress and plane strain fracture are qualitatively the same and the appropriate yield stresses differ only to the extent that they fall on different parts of the shear failure locus. In thermoplastics, however, plane strain crack propagation occurs through the formation and breakdown of crazes [12]. Associated with craze formation is a stress locus that differs radically from the yield locus associated with shear plasticity in the same materials. This is probably true also of the craze breakdown locus versus the ultimate stress locus for shear flow but no information in this regard is known.

(5) Yield, strain hardening, and fracture characteristics vary considerably from one material to another. For example, as illustrated in Fig. 2a, necks formed under uniaxial loading are unstable in many ductile metals with the result that deformation is largely confined to a length in the gauge section equal to its thickness. As pointed out by Tetelman and McEvily the plastic work to fracture should then be proportional to the thickness squared. With this kind of material G_C obtained from the Dugdale test should show a linear dependence on sheet thickness that is predictable. By contrast if a material strain hardens sufficiently with strain so that a stable neck forms (Fig. 2b) the length of specimen to undergo deformation bears a very different (if any) relation to its width. For example, BPA polycarbonate strain hardens

and forms stable necks in this manner (e.g. see [13] Fig. 11.40) and, as the following section describes, the length of specimen to undergo plastic deformation ahead of the crack tip during ductile failure is several times as great (in the stress direction) as the sheet is thick. Given the complexities of these phenomena, particularly as affected by stress state, it is unrealistic to expect that the thickness dependence of Dugdale G_C's will provide a good estimate of the thickness dependence of shear lip energies.

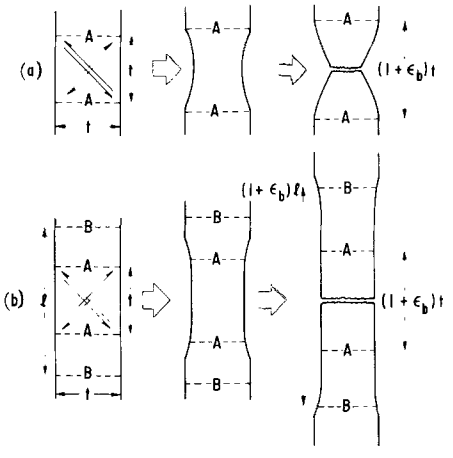

Figure 2 Failure geometries of ductile materials in which (a) insufficient strain hardening results in an ultimate engineering stress σ_u lower than the yield stress σ_y and (b) sufficient strain hardening results in $\sigma_u > \sigma_y$.

2. Dugdale experiments with BPA polycarbonate sheets

Dugdale tests have been conducted here on sheets of Lexan®* BPA polycarbonate of thicknesses from 0.001 to 0.085 in. Resin $[\eta] \simeq 0.6\,\mathrm{dl\,g^{-1}}$ in all cases but one (for 0.0036 in. thick film $[\eta] = 1.0\,\mathrm{dl\,g^{-1}}$). Specimen characteristics are given in Table I. Thick films and sheets specimens were pulled to failure with custom-built 7 in. wide grips at a crosshead rate of 0.05 in. $\mathrm{min^{-1}}$. The positions of the crack and plastic zone tips were noted by eye with the aid of scale scribed on the specimen surfaces. In all tests but one specimens of the films thinner than 0.010 in. were step-loaded to failure; specifically, a weight was hung for one minute from a 10:1 lever arm attached to one of the specimen chucks. The weight was removed and the crack and zone tip positions then measured with a travelling telemicroscope. The next larger weight was then applied for 1 min and so on.

* General Electric trademark

Up to a sheet thickness of 0.015 in. all specimens obeyed the Dugdale model reasonably well and catastrophic failure developed at or just beyond the point of maximum load (see Fig. 3). With the shorter specimens 0.015 in. thick and greater (Figs. 4 and 5) a broad load maximum was observed but failure was not catastrophic. Rather the crack propagated gradually through the remainder of the specimen at a rate that usually accelerated somewhat at first. Nevertheless, data obtained as the load maximum was approached fell on the Dugdale curve. Finally, two 0.062 in. thick specimens of much greater length were tested; they failed catastrophically, which indicates that non-catastrophic failure is only a result of insufficient total elastic displacement. That is, if crack opening displacement equals the total elastic displacement of the specimen (because its length is small) tensile failure will not become catastrophic.

Following Brinson, G_C has been calculated for all specimens according to the Dugdale–Goodier–Field expression modified for specimen width and yield stress effects

$$G_C = (8\sigma_y^2 s_C/\pi E)\gamma^2 \qquad (2)$$

where σ_y is the tensile yield stress of the sheet, s_C is the length of the plastic zone ahead of the crack tip at the maximum load attained and E is the tensile modulus. γ is a factor introduced to correct for the fact that specimen width is not infinite and the maximum load is an appreciable fraction of the yield load. Following Brinson appropriate values of γ were taken from Forman [14], and are listed in Table I.

The values of G_C thus calculated for thicknesses greater than 0.015 in. are to be regarded with some reservation of course because of the serious deviations seen in plots such as Fig. 5 and because most of these failures were not catastrophic. Independent estimates of G_C were thus made according to

$$G'_C = \sigma_y \Delta t \qquad (3)$$

where Δt is the plastic displacement at the crack tip at the point of maximum load. Δt was calculated from the strain ϵ_p in the plastic zone and its dimension t in the stress direction: $w/w_0 = (1 + \epsilon_p)^{-1}$, $t = t_0 + \Delta t = t_0(1 + \epsilon_p)$ where w and w_0 are the measured thicknesses of the sheet in the zone and outside the zone and t_0 is the "gauge

TABLE I Characteristics of Dugdale specimens

Specimen dimensions (in.)			History[b]	Notch	Tensile properties[d]			Plastic zone dimensions[e](in.)			γ^{2}[f]
Thickness	Width	Length[a]		type[c]	σ_y(psi)	ϵ_b(%)	ϵ_p(%)	w	t	s	
0.0013	1.5	3.25	1	CN	6750	26	34	0.00106	0.0338	0.0943	1.30
0.0036	1.5	3.25	4	DEN	7200	42	58	0.0024	0.025	0.154	1.10
0.0055	6.1	10.50	1	CN	7770			0.0030	0.048	0.31	1.28
0.0057	1.5	3.25	1	CN	6900	95	138	0.00376	0.0205	0.118	1.25
0.0102	7.0	6.3	1	CN	7260	95	85	0.0060	0.075	0.50	1.30
0.0159	5.4	4.1	3	CN	7580			0.0095	0.081	0.37	1.32
0.0160	7.0	6.3	1	CN	7780	128	97	0.0094	0.125	0.37	1.72
0.0189	4.0	4.1	3	CN	9110			0.011	0.067	0.22	1.30
0.0210	7.0	6.3	1	CN	7820	98	93	0.0123	0.069	0.39	1.46
0.0300	7.0	6.3	1	CN	8370	173	87	0.019	0.100	0.40	1.26
0.0475	7.0	6.3	1	CN	9320	94	100	0.030	0.066	0.45	1.30
0.0620	7.0	11.0	1	CN	8830	109	83	0.040	0.070–0.100	0.47	1.85–2.1
0.0620	6.4	11.4	2	CN	9330	111	78	0.041	0.093	0.35	1.61
0.0854	7.0	11.0	1	SEN	9110	118	88	0.050	0.110	0.65	1.21
0.0854	7.0	2.8	1	CN				0.050	0.136	0.77	1.39

(a) Length between chucks.
(b) 1 = As-extruded, loaded in extrusion direction; 2 = extruded, annealed at 170° C, cooled to 140° C and air-quenched; 3 = as-compression moulded; 4 = solvent cast.
(c) CN = centre notch, DEN = double edge notch, SEN = single edge notch.
(d) Specimen cut from Dugdale specimen after test with long axis parallel to original loading direction, ϵ_b = machine elongation at break divided by nominal gauge length, ϵ_p = plastic strain in neck calculated from reduction in crossectional area, σ_y = yield stress.
(e) Measured at point corresponding to maximum load during Dugdale test; w = sheet thickness, t = dimension in loading direction, s = length from crack tip to zone tip.
(f) G_C correction factor.

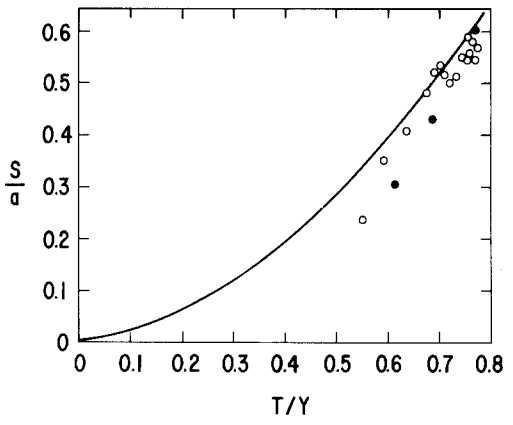

Figure 3 Comparison of plastic zone length in 0.015 in. thick film to theoretical prediction based on Dugdale model. s = zone length, a = zone length plus half the crack length, T = applied load, Y = yield load. ○, • data before and after load maximum respectively.

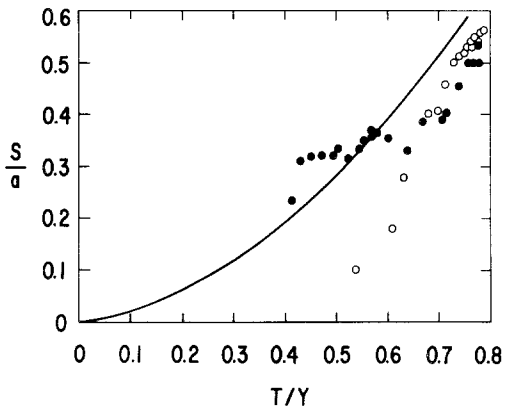

Figure 4 Comparison of plastic zone length in 0.020 in. thick film to Dugdale prediction. ○, • data before and after load maximum respectively.

length" of specimen to be plastically deformed.

Values of G_C and G'_C are plotted versus sheet thickness in Fig. 6. For most specimens the agreement between G_C and G'_C is reasonably good which suggests that G_C calculations from equation 2 are valid even when deviations from theoretical behaviour are appreciable, as in Fig. 5. The sheet thickness dependence of G_C is very pronounced from 0 to 0.015 in. The drop between 0.015 in. and 0.020 in. is superficially suggestive of the G_C behaviour observed for 7075-TG aluminium alloy when the transition from slant fracture to plane strain failure occurs. However, in the present case no qualitative difference between the thin and thick specimens in the morphologies of yield zones and fracture surfaces was casually evident, nor is

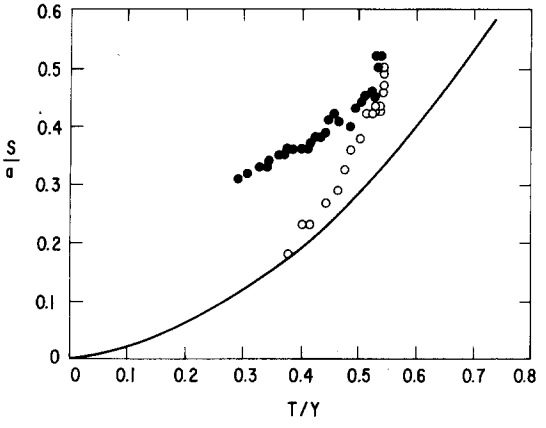

Figure 5 Plastic zone lengths versus Dugdale prediction for 0.030 in. thick sheet. ○, ● data before and after load maximum respectively.

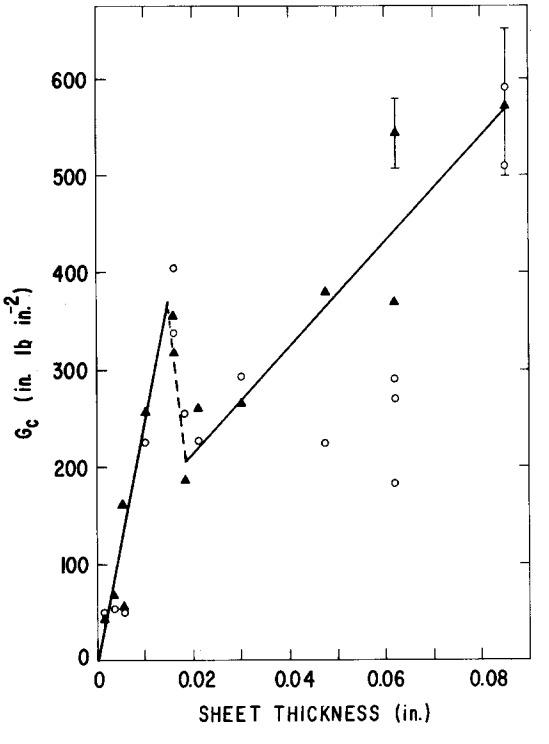

Figure 6 G_C (▲) and G'_C (○) versus Dugdale specimen thickness w.

G_C independent of thickness above 0.020 in. as would be the case if $G_C = G_{IC}$ in this range.

The complex thickness dependence of G_C is a reflection of changes in failure zone geometry rather than a complete artifact of, for example, specimen geometry and crack dimensions. Support for this conclusion is seen in Fig. 7 where t, ϵ_p and s are plotted versus sheet thickness. For each of these a maximum is evident between 0.010 and

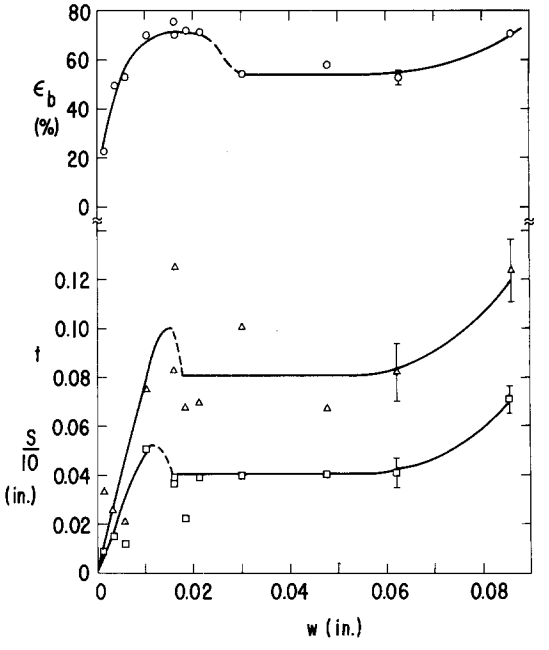

Figure 7 Dugdale plastic zone dimensions versus specimen thickness. Respectively t, and ϵ_p are the plastic zone size in the applied stress direction and the corresponding plastic strain. s is the zone length (direction of crack propagation).

0.020 in. (It is also notable that initially $dt_0/dw = 4$ rather than 1, the value to be expected if a stable neck did not develop.)

The source(s) of the complex behaviour seen in Fig. 7 is not currently clear. (Differences in stress axiality and geometry at the crack tip are likely suspects). It is conceivable that something like a plane stress/plane strain transition occurs in the strain-hardened material of the plastic zone. For the primary purpose of this paper it is sufficient to note that (a) ϵ_p is 50 to 70% for the most part, and (b) that t and s rise abruptly from zero at zero thickness apparently to maxima; these maxima are followed by broad plateaus. The result however, is the complex dependence of G_C on thickness seen in Fig. 6.

Finally, the experimental requirements for characterizing G_C in a fully valid way for the thicker films and sheets are worth noting. The wide specimen grips were built specifically to allow use of unusually wide specimens in order to counteract problems associated with gross plasticity. Even with these widths, however, unusual specimen lengths were required with sheet thicknesses above 0.015 in. in order to continue to achieve catastrophic failure.

3. A single groove double cantilever beam specimen for assessing shear lip formation energies

For several reasons indicated above a type of specimen differing from the Dugdale tensile specimen is needed for the assessment of the formation energies of shear lips, especially thick ones and/or ones formed at high speeds. A double cantilever beam specimen which is useful in this assessment is described below.

3.1. Specimen Geometry

The geometry of the DCB specimen used here to assess shear lip formation mechanics is diagrammed in Fig. 8. It differs from the standard G_{IC} cleavage specimen, used first by Berry [10] for thermoplastics, in having only one side groove. This groove is sufficient to constrain the crack to the desired plane. The absence of a groove on the opposite face allows shear deformation to occur in a plane *normal* to the groove direction.

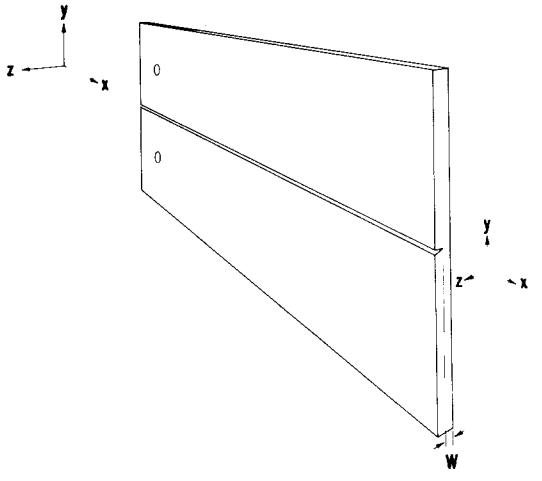

Figure 8 Double cantilever beam specimen with single V-shaped groove.

Specimens with grooves of different crossectional shapes have been used. The values of G_C obtained depend on groove shape in minor ways only. At first the grooves consisted of parallel sided saw cuts, the cut thickness being 0.010 and 0.025 in. Subsequently V grooves (as in Fig. 8) were used, a few with root radii of 0.010 and 0.005 in. and most with root radii of 0.001 in. The angle of the V in all cases was 27°. Specimens with widths of 2 and 3 in. lengths of 6 to 12 in. and thicknesses of 0.125 to 0.50 in. have been tested.

Several effects of specimen geometry on the outcome of the test have been seen as follows: (1) general yielding of the arms occurs, as expected, when their moments of inertia are small compared to net section thickness w (more precisely, to the level of G_C); (2) lateral buckling tendencies can be severe, the more so the smaller the ratio of total specimen width to net section thickness; for a given ratio buckling becomes a greater problem with increasing crack length; (3) the net section thickness beyond which plane strain failure (craze formation and fracture) begins at the root of the groove depends on groove shape and specimen width. The greater the b/w ratio, and the sharper the groove (i.e. smaller groove angle or smaller radius of curvature) the greater is the tendency for plane strain failure. We have avoided or minimized these problems through trial and error rather than by quantitative analyses.

3.2. Materials

Most of the tests have been conducted on as-extruded sheets of Lexan 9034 BPA polycarbonate, a ultraviolet stabilized grade of $[\eta] = 0.62\ \mathrm{dl\,g^{-1}}$. Sheet thicknesses of 0.129, 0.200 and 0.50 in. have been used. Results of tests on copper and aluminium will be reported later.

3.3. Test Procedure

Subsequent to the cutting of the side groove, holes for the loading pins were drilled through one end of the specimen, each hole being located about $\frac{1}{2}$ in from the end and midway between the groove and the top or bottom edge of the specimen (Fig 8). A starter "crack" was sawn through the specimen from the end to a position usually about 1 in. beyond the centre line between the loading holes. The controlled propagation of plane strain cracks from inserted cuts in thermoplastics usually requires a sharpening of the inserted cut because the true crack tip is sharper than the cut. This was not required in the present set of experiments because the plastic zone at crack tip was larger in all cases than the starter saw cut.

However, as mentioned above a serious buckling tendency exists. This is augmented by the large values of G_C encountered and the inherent asymmetry of the single groove cleavage specimen. When the crack is long enough the loaded ends of the specimen tend to twist out of the original specimen plane and the failure tends to take on a Mode III character. The buckling was countered by fashioning a constraining yoke for the specimen. The yoke was formed of two $\frac{1}{2}$ in. thick poly-

carbonate sheets, each 6 in. x 10 in. in area; bolts at the four corners of the yoke were adjusted so that the internal spacing was slightly greater than the thickness of the specimen to be tested. The yoke was then slid over the free end of the specimen and up to a position about 1 in. from the loading pins. The extra lateral stiffness provided by the yoke countered buckling well enough to allow tests to be run over sufficient ranges of w and c. Although the countering of the buckling tendency produced friction between the yoke and the specimen the frictional force was never more than a few percent of the total force required for crack propagation.

The specimens were loaded in an Instron tester at a constant cross-head rate, usually 0.05 in. min^{-1}. (Results for polycarbonate, obtained at rates up to 200 in. min^{-1}, will be reported in a subsequent paper.) When plane strain crack propagation occurs under these conditions the strain energy release rate G_C is usually given as

$$G_C = \frac{f^2}{2w}\frac{d(\delta/f)}{dc}$$

where f is the applied force and δ the cross-head displacement. In the case of double cantilever beams of constant width the beam compliance δ/f is proportional to the crack length raised to a power, namely

$$\delta/f = \alpha c^n$$

with n found empirically [10] to be < 3. Thus $d(\delta/f)/dc = n\delta/fc$ and $G_C = nf\delta/2wc$. This expression although first derived [10] for conditions of constant displacement is thus applicable to constant rate conditions as well.

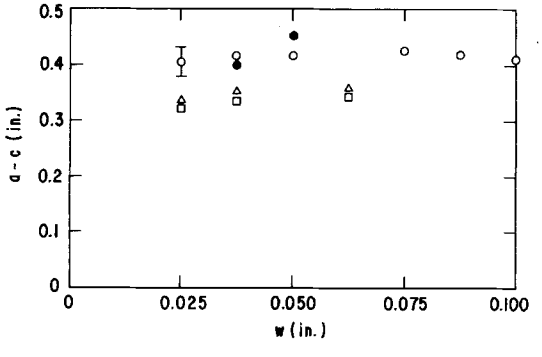

Figure 9 Dependence of length of plastic zone at surface on net section thickness in S-G DCB specimens. 2 in. wide specimens: □ 0.001 in. groove radius, △ 0.005 in. groove radius. 3 in. wide specimens: ○. Solid points measured while specimen under load. Open points measured after specimen unloaded.

In most plane strain cleavage experiments the length of the plastic zone ahead of the crack is negligible compared to the crack length and the quantity $f\delta/c$ is constant over most of the length of the specimen [10]. In the studies reported here $f\delta/c$ decreased gradually with increasing c (c being the length of crack evident on the ungrooved face of the specimen) albeit the dependence of $f\delta/c$ on c lessens with increasing c. We found, however, that the quantity $f\delta/a$, where a is the distance from loading pins to tip of the plastic zone on the ungrooved specimen surface, is more nearly independent of crack length. (On the average a-c is 0.3 to 0.4 in. for these polycarbonate specimens, Fig. 9.) Correspondingly, n has been determined as $d \log (\delta/f)/(d \log a)$ using δ, f and a data from the crack propagation experiments. We found such log–log plots to be linear with $n = 2.5 \pm 0.1$. With this value of n the strain energy release rate was calculated as

$$G_C = nf\delta/2aw.$$

Aside from the *a posteriori* observation that $f\delta/a$ is less dependent on crack length than $f\delta/c$ there are two reasons that support the use of a in place of c in calculating G_C. First, as will be developed in the next section, the crack front at the specimen surface lags the crack front at the root of the groove by a distance almost equal to a-c; thus, the choice a is nearly as valid as the choice of c for this reason alone. Second, most theoretical analyses (e.g. see Liu [15] p. 25) consider that the plastic zone is effectively an extension of the crack.

4. Results for DCB specimens

Values of $nf\delta/2aw$ are plotted versus a in Fig. 10 for all of the 3 in. wide, 8 in. long, 0.001 in. radius V groove polycarbonate specimens tested, and in Fig. 11 for all of the 2 in. wide, 6 in. long specimens tested; these contained 0.001 and 0.005 in. radius V grooves as indicated. In each case little or no dependence on a (and thus c) is seen from $a \simeq 1.5$ to 4.5 in. For $a > 4.5$ in. $nf\delta/2aw$ usually begins to decrease. Following Berry this deviation is attributed to the proximity of the end of the specimen: entrance of the crack tip into this region brings deviation from the stiffness versus crack length relationship.

In Fig. 12 values of G_C taken at $a = 3.8$ in. from Figs. 10 and 11 are plotted versus w. Taking

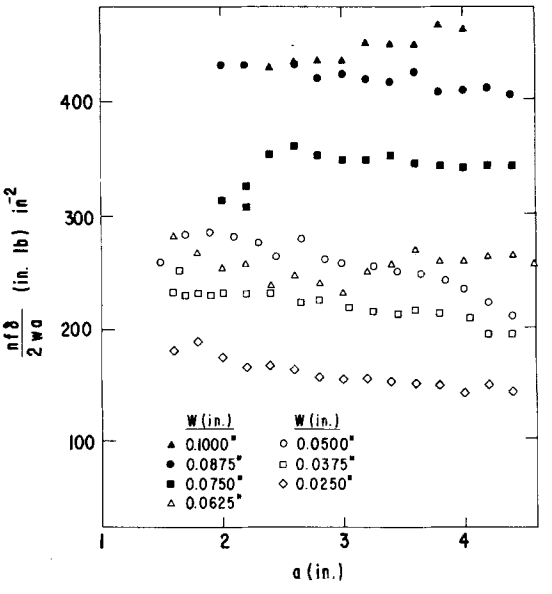

Figure 10 Dependence of $nf\delta/2aw$ on a for 3 in. × 8 in. S-G DCB specimens containing 0.001 in. V grooves. Net section thickness w as shown.

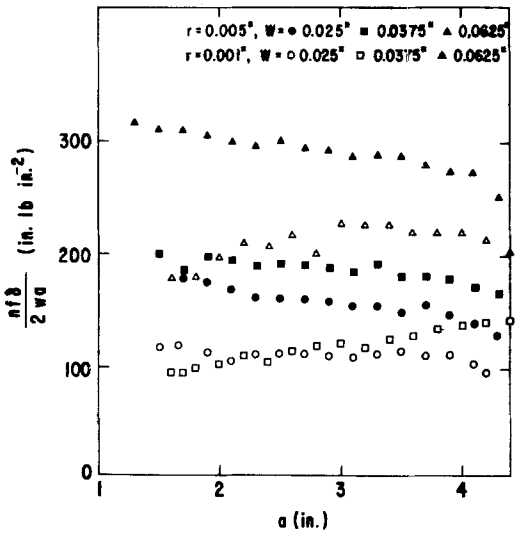

Figure 11 Dependence of $nf\delta/2aw$ on a for 2 in. × 6 in. S-G DCB specimens containing 0.001 in. and 0.005 in. V grooves.

all values at the same large value of a was done for two reasons. First a-c has usually become less than 10% of a at this point so that errors in G associated with an incorrect choice of crack tip position will be small. Second the crack velocity which depends on crack length will be essentially the same in all cases (about 0.4 in. min^{-1} at a = 3.8 in.).

Results for the V groove specimens fall approximately on a single straight line initiating at the origin. If significant at all, the small apparent deviations of the values obtained from the 2 in. × 6 in. specimens containing 0.001 in. radius V grooves are conceivably due to a difference in specimen axis orientation relative to the sheet extrusion direction: the 3 in. wide specimens were cut so that their long axes all coincided with the extrusion direction. The orientation directions of the 2 in. wide specimens, cut and used earlier in the programme are not known. (In any case, these sheets exhibit very little change in relative lateral dimensions when annealed at 170° C for several hours. Thus the average degree of anisotropy in the sheet plane is small.)

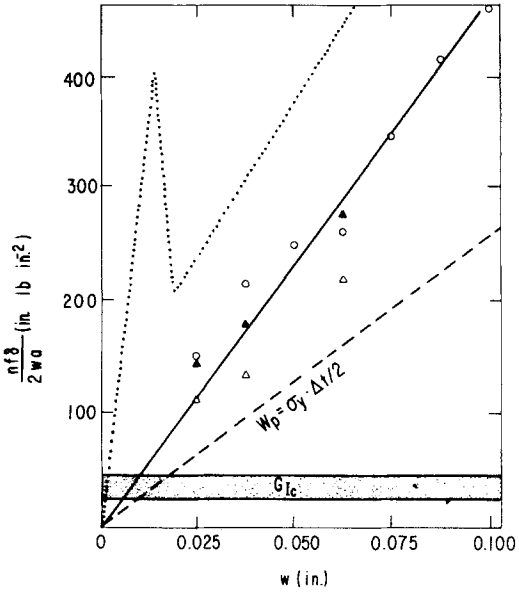

Figure 12 G_C at a = 3.8 in. from Figs. 10 and 11 versus net section thickness w. Dotted line: thickness dependence of Dugdale G_C from Fig. 6.

Although not shown, values for the 0.025 in. saw cut specimens fall on a higher, nearly parallel line that extrapolates to $G_C \simeq 130$ at $w = 0$. (The reason for this non-zero extrapolated value is a plastic zone that is shaped differently at its base from those arising from V grooves.)

K_{IC} values of 2000 to 3500 psi $in.^{1/2}$ have been reported previously for polycarbonate [8, 16, 17]. For the sheets used by us G_{IC} from double grooved DCB specimens lies between 26 and 47 in. lb $in.^{-2}$ at low crack velocities. (These values correspond to $K_{IC} = 3000$ to 4000 psi $in^{1/2}$.) Since G_{IC} is not a function of w, these values are used as the bounds of a horizontal G_{IC} band superposed on Fig. 12.

Finally, the Dugdale G_C curve from Fig. 6 is superposed on Fig. 12 for contrast. The initial thickness dependence of the Dugdale G_C is about eight times greater than the thickness dependence of the S-G DCB G_C. The sources of this difference are the different sizes of, geometries of, and plastic strains in the respective plastic zones, as will be developed below.

As noted earlier polycarbonate shear lips 0.050 and 0.010 in. wide have developed during slow fracture of ungrooved specimens 0.5 in. thick. By contrast cracks have been propagated in single groove specimens up to 0.250 in. thick containing net sections up to 0.150 in. thick with no sign of plane strain failure. The onset of plane strain fracture for $w \geqslant 05$ to 0.10 in. appears to require a greater specimen thickness and a sharper, deeper groove. The evidence for this conclusion comes from an experiment to be detailed following a description of the plastic zone.

(Fig. 13b) the crack front and the root of the side groove form an acute angle α that increases with w; a value of roughly 15° is typical however. Thus the internal crack tip, at the root of the groove, leads the external crack tip by a distance that approaches the length of the tines of the plastic zone.

Transverse sections were cut with a band saw through the arms of all the tested cleavage specimens. From low power photomicrographs of the faces of these sections accurate determinations were made of the plastic zone thicknesses at the specimen surfaces and the paths of the cracks from the root of the groove to the free surface. Determinations of the plastic displacement at the surface, Δt, in the loading direction, were made from comparison of these photomicrographs with photomicrographs of similar sections through undeformed grooves.

Two diagrammatic cross-sections of a specimen

Figure 13 S-G DCB plastic zone and crack front. (a) Appearance on ungrooved specimen surface and sectional views. (b) Cross-section in groove midplane showing crack front. (c) Superposed cross-sections normal to crack propagation direction at C-C (heavy solid line) and at A-A (dotted line). Axes are same as in Fig. 8.

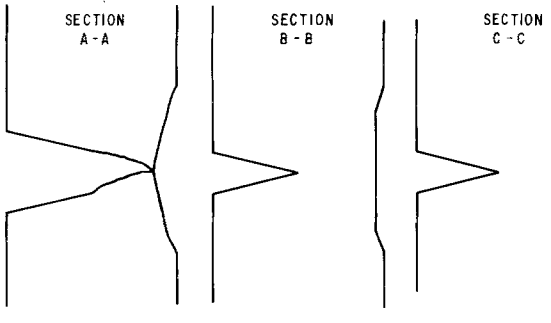

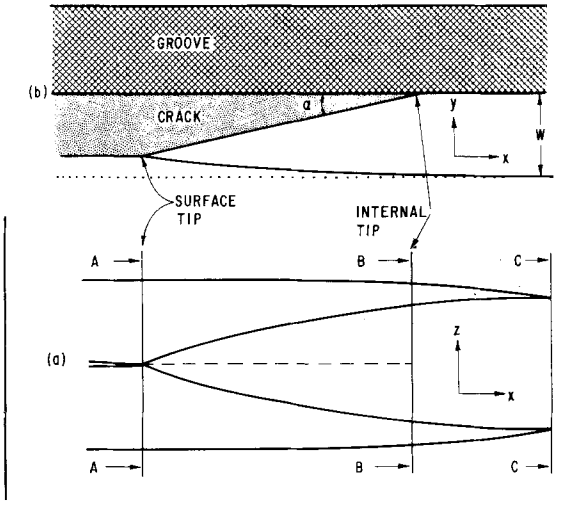

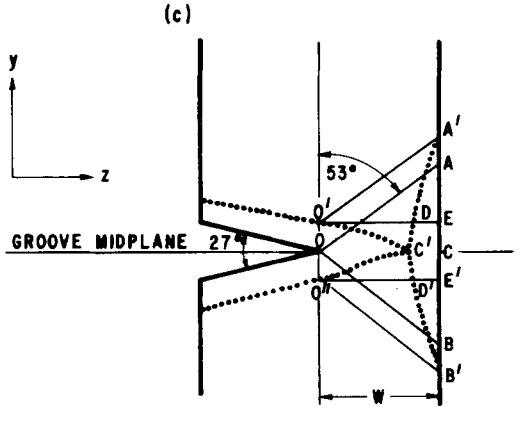

5. Plastic zone geometry and strain

The geometry of the crack front and plastic zone in the single groove DCB specimen (Fig. 13) differs substantially from that in a polycarbonate Dugdale specimen. Viewed from the ungrooved side (Fig. 13a) the plastic zone at the surface looks like a two-tined spear, each tine lying above or below the plane containing the edge of the crack. Each tine thickens, primarily by the yielding of the adjacent material *inside* of the tines. The zone halves meet slightly in front of the surface edge of the crack. The similarity to the zone shape in Fig. 1 is clear.

Viewed normal to the midplane of the groove

normal to the root of the groove are superposed in Fig. 13c. The sections may be viewed as located just in front of the surface tips of the plastic zone (section C-C of Fig. 13a) and just behind the external crack tip (section A-A of Fig. 13a). The plastic zone tips at A and B are located respectively, above and below the groove midplane by a distance $AC = BC = t_0/2$. In the section corresponding to the position of surface crack tip in Fig. 13a and b; the surface boundaries of the plastic zone lie respectively at a distance $A'C = B'C = t/2$ above and below the midplane. The crack (which in the view shown in Fig. 13c can be said to have "initiated" at the groove root) has grown out and reached the surface at C′ along a path that sometimes deviates from the groove midplane. Because of the constraint produced by the groove the integrated plastic displacement in the loading direction O′C′D plus O″C′D′ is compensated for entirely by the integrated lateral displacement of the ungrooved specimen surface A′DE plus B′D′E′. The lateral surface displacement is a maximum CC′ at about the groove midplane.

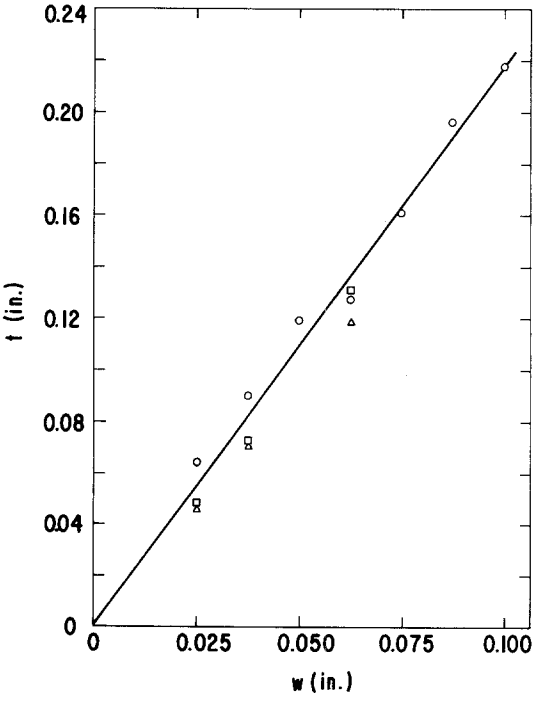

Figure 14 Dependence of S-G DCB plastic zone thickness t at specimen surface on net section thickness w.

From examination of V groove specimens of w from 0.025 to 0.100 in. it was found that both t and Δt were proportional to w. Variation in t with w is shown in Fig. 14. The ultimate surface plastic strains in the loading direction $\epsilon_{p,s} = \Delta t/(t - \Delta t)$ are thus independent of w, having an average value of about 30% for both groove configurations (Fig. 15).

From the lack of dependence of $\epsilon_{p,s}$ on w it is reasonable to infer that in each specimen the plastic strain in the interior is equal to that on the surface. (This inference is supported by measurements of birefringence distribution in the yield zone to be discussed in a subsequent paper.)

Since t and Δt have the same linear dependence on w, a simple model can be constructed that rationalizes the observed dependence of G_C on w. The gauge length of each element to be strained can be supposed to have its ends on the lines OA and OB (Fig. 13c). Thus averaged over the thickness w the original length and ultimate displacement of these elements are $t_0/2$ and $\Delta t/2$ respectively.

Advance of the crack by a unit of length in the x direction (Fig. 13a and b) is equivalent to cracking through a transverse section, as in Fig. 13c of unit thickness. Assuming the material to be an ideal elastoplastic having an ultimate engineering stress σ_u equal to the plane strain yield stress σ_y, the plastic work w_p required to advance the crack per unit length and per unit of width w is

$$w_p = \sigma_y \Delta t/2.$$

Yee and Olszewski [18] have determined the ultimate properties under plane strain conditions of the sheet used in these cracking studies. The specimens were 4 in. long, 2 in. wide and 0.125 in. thick. Gauge sections had nominal lengths of 0.040 in. The plane strain yield stress is 10 600 psi and the ultimate plastic elongation as calculated from the reduction in gauge thickness is 100%. Using their value of yield stress, w_p was calculated for each of the V groove specimens. On the average w_p is 60% of the corresponding experimental value of G_C (Fig. 12).

6. Requirements for determination of shear lip size

The failure mechanism for the single groove DCB specimens is one in which shear flow occurs in a plane transverse to the direction of crack propagation. The deformed region, left on the fracture surface has a geometry identical to that of shear lips. It thus appears possible to use data from

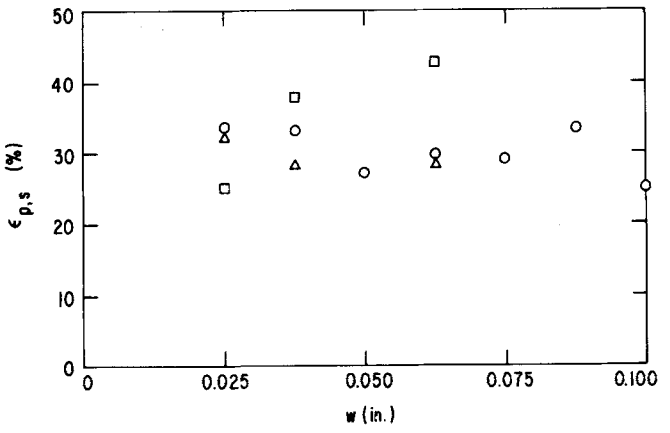

Figure 15 Dependence of S-G DCB surface plastic strain $\epsilon_{p,s}$ on net section thickness w.

transverse "plane strain" crack propagation experiments, as in Fig. 12, to assess the energy of formation of shear lips of given widths.

However, the experimental method as described so far is inadequate for predicting shear lip widths. For example, the failure of all single V-groove DCB specimens of thicknesses up to 0.250 in., containing net sections up to 0.150 in. has occurred completely by the transverse plane strain mechanism. These net section widths exceed the widths of the polycarbonate shear lips produced in the slow cracking of ungrooved 0.5 in. thick sheets by 0.05 to 0.100 in.

The onset of conventional plane strain cracking (i.e. fracture by the crazing mechanism) at $w = 0.05$ in. occurs in S-G DCB specimens having greater thicknesses and deeper narrower grooves than described here. In experiments to be described in a subsequent paper, fracture specimens having parallel-sided grooves 0.010 in. thick have been fashioned from sheets 0.5 in. thick. Transverse plane strain failure is the sole mechanism of failure up to $w \simeq 0.05$. At this value of w (which corresponds to the shear lip width in specimens 0.5 in. thick) the craze breakdown mechanism begins at the root of the groove. Presumably in these specimens a greater level of tensile stress in the z direction exists below the root of the groove. As a consequence the hydrostatic tension is raised relative to the resolved shear stress. It is evident that this sensitivity of failure mode to groove shape and specimen thickness implies that the criterion for shear lip size is a stress criterion rather than an energy criterion. The operative criterion will probably be based on the shear yield locus and the craze fracture locus in stress space.

7. Conclusions

Both Dugdale specimens and single groove double cantilever beam specimens of BPA polycarbonate give thickness-dependent values of G_C. With S-G DCB specimens the dependence is linear throughout the range tested. With Dugdale specimens the dependence is initially linear but more complex above a thickness of 0.015 in. For the initial linear range of the Dugdale G_C-w plot $\partial G_C/\partial w$ is eight times that for the corresponding S-G DCB plot. This difference in initial thickness dependence arises mostly from the differences in plastic strains (50 to 70% versus 30%) and average "gauge lengths" (a ratio of about 7 to 1 for a given net section thickness) for the plastic zones of the respective specimen types. Presumably these differences in turn arise from a difference in the level of the hydrostatic components of stress operative in each type caused by the difference in specimen geometry.

In any case the S-G DCB specimen appears to be superior to the Dugdale specimen for assessing shear lip formation energies in terms of the geometries and strains of the plastic zones. Moreover, the onset of plane strain failure at the root of the groove in the S-G DCB specimen can be made to occur at a net section thickness equal to the shear lip width if the groove profile is sufficiently sharp. Finally, the S-G DCB specimen can yield values of G_C as a function of crack velocity, an advantage in assessing shear lip formation energies under impact conditions.

Acknowledgements

The authors wish to thank A. S. Argon, L. F. Coffin, Jr, D. Lee, G. P. Marshall and J. G.

Williams for enlightening discussions and C. F. Pratt and W. V. Olszewski for help with the Dugdale measurements. We are also indebted to A. F. Yee and W. V. Olzewski for permission to use their unpublished plane strain yield stress results.

References

1. A. S. TETELMAN and A. J. MCEVILY, Jr. *"Fracture of Structural Materials"*, (Wiley, New York, 1967).
2. D. S. DUGDALE, *J. Mech. Phys. Solids* 8 (1960) 100.
3. J. N. GOODIER and F. A. FIELD, in *"Fracture of Solids"*, Metallurgical Society Conference Vol. 20, edited by D. C. Drucker and J. J. Gilman (Interscience New York, 1963) p. 103.
4. J. E. STRAWLEY and W. F. BROWN, Jr., in *"Fracture Toughness Testing and its Applications"*, ASTM Special Technical Publication No. 381 (American Society for Testing and Materials, Philadelphia, PA, 1965) p. 144.
5. J. F. KNOTT, *Mat. Sci. Eng.* 7 (1971) 1.
6. V. WEISS and S. YUKAWA, in *"Fracture Toughness Testing and its Applications"*, ASTM Special Technical Publication No. 381 (Americal Society for Testing and Materials, Philadelphia, PA, 1965) p. 14.
7. J. A. MANSON and R. W. HERTZBERG, *Crit. Rev. Macromol. Sci.* **1** (1973) 433.
8. P. L. KEY, Y. KATZ and E. R. PARKER, UCRL-17911, Lawrence Radiation Laboratory, University of California, Berkeley, California, February 1968.
9. H. R. BROWN and I. M. WARD, *J. Mater. Sci.* 8 (1973) 1365; J. S. HARRIS and I. M. WARD, *ibid*, 1655.
10. J. P. BERRY, *J. Appl. Phys.* **34** (1963) 62.
11. H. F. BRINSON, *Proc. Soc. Exp. Stress Anal.* **27** (1970) 72.
12. R. P. KAMBOUR, *J. Polymer Sci. Macromol. Rev.* 7 (1973) 1.
13. R. P. KAMBOUR and R. E. ROBERTSON, in *"Polymer Science"*, edited by A. D. Jenkins (North Holland, Amsterdam, 1972) Chapter 11.
14. R. G. FOREMAN, *J. Basic Eng.* 88 (1966) 82.
15. H. W. LIU, in *"Fracture Toughness Testing and its Applications"*, ASTM Special Technical Publication No. 381 (American Society for Testing and Materials, Philadelphia, PA, 1965) p. 25.
16. A. P. GLOVER, F. A. JOHNSON and J. C. RADON, *Polymer Eng. Sci.* **14** (1974) 420.
17. M. PARVIN and J. G. WILLIAMS, *J. Mater. Sci.* **10** (1975) 1883.
18. A. F. YEE and W. V. OLZEWSKI and S. MILLER, *"Symposium on Toughness and Brittleness in Plastics"* Am. Chem. Soc. Advances in Chemistry Series, in press.

Received 8 October 1975 and accepted 30 October 1975